# Effect of the wall roughness on slip and rheological properties of hexadecane in molecular dynamics simulation of Couette shear flow between two sinusoidal walls

A. Jabbarzadeh, J. D. Atkinson, and R. I. Tanner
*Department of Mechanical & Mechatronic Engineering, The University of Sydney, NSW 2006, Australia*
(Received 24 May 1999)

Molecularly thin liquid films of alkanes in extreme conditions in a boundary lubrication regime have been investigated. The wall is modeled as a rough atomic sinusoidal wall. The effect on the boundary condition of the roughness characteristics, given by the period and amplitude of the sinusoidal wall, is studied here. The effect of the molecular length of the lubricating fluid is also examined here. The results show that the relative size of the fluid molecules and wall roughness determines the slip or nonslip boundary conditions. The effect of wall roughness characteristics on the rheological properties of the lubrication film is also studied.

PACS number(s): 83.20.Lr, 02.70.Ns, 83.50.Ax, 83.20.Jp

## I. INTRODUCTION

The boundary conditions relevant to flowing fluids are very important in predicting fluid flows in many applications. According to the findings of modern tribology, in the thin-film lubrication regime the thickness of the lubricating film reaches molecular dimensions and nanometer scales [1]. For these ultrathin films it is very difficult to determine the boundary conditions and fluid properties by experimental measurement. In these thin films the expected shear rates can be very high and beyond the values that can be studied in laboratories. Molecular-dynamics (MD) simulations, however, have proved to be an efficient method in investigating these complex systems at high shear rates and extreme conditions.

The surfaces that are considered in most molecular simulations and theoretical analyses are idealized smooth surfaces. Slip on the wall has been studied by MD simulations by Thompson and Robbins [2] and Thomson, Grest, and Robbins [3] for spherical and linear molecules. We have also studied the slip for spherical Lennard-Jones particles [4] and more complex molecules of hexadecane [5,6]. Similar to the results obtained by Thompson and his colleagues, we have observed significant slip that depended on many factors such as wall energy and shear rate. In our works we have studied the effect of wall properties such as wall energy and wall type on the slip and rheological properties of the lubricant film. Also detailed studies have been conducted on the fluid film structure and molecular orientation, where we have discussed in detail the results and their relevance to current experimental work. However, in all the mentioned MD simulations the characteristic length scale of the roughness for the solid surfaces was in the order of the atomic spacing of the solid lattice structure. These smooth surfaces do not occur in most practical applications and some kind of roughness with longer scales should be considered. The current paper focuses on the effect of physical roughness greater than the atomic spacing and seeks to experiment on the effect of this roughness and its characteristics and also of the molecular size of the lubricant film on the boundary conditions. The roughness of a surface depends on the material and the method used for preparing the surface and ranges from many microns to nanometers. However, in experiments [7] for studying microscopic scale friction, surfaces with roughness ranging from 0.2 to 50 nm are used. In the current paper we will study surfaces with a roughness length scale in the order of nanometers, which is feasible to simulate by MD.

It has been suggested [8] that in discussing a flow near a solid surface, three length scales should be considered: (a) A length scale ($L_m$) depending on the microstructures making up the fluid; (b) a length scale ($L_r$) depending on the roughness of the surface; and (c) a length scale ($L_g$) depending on the geometry of the flow such as film thickness or tube diameter. A discussion by Pearson and Petrie [9] had previously suggested that the boundary condition of flow near a solid surface depends on the relative size of the fluid particles, surface asperities, and characteristic dimension of flow such as tube diameter or film thickness. Three distinct cases are possible considering the mentioned length scales.

(i) $L_g \gg L_r \gg L_m$ is a condition that happens for fluids with small molecules. In this case because of the small scale of the asperities, the Reynolds number is low and the viscous forces are dominant near the boundary. According to Richardson [8], regardless of the wall adhesion in large scales ($L_g$) an apparent nonslip condition prevails even if slip happens in the $L_r$ scale.

(ii) $L_g \gg L_m \gg L_r$ is a condition typical of coarse powders with smooth surfaces. An example of this case is the movement of sand in a tube. In this case slip is often seen on the wall.

(iii) $L_g \gg L_r \approx L_m$ is typical of the flow for a large molecule fluid near surfaces with roughness comparable with the size of the molecules. In this case slip often depends on the chemical or mechanical adhesion.

In practice, a solid surface contains roughness elements which are distributed randomly on the surface, but we adopt a simplified model in the form of transverse sinusoidal roughness with an average roughness length scale.

Experimental measurements by scanning tunneling microscopy (STM) techniques for typical surfaces such as gold and mica give a roughness measured from peaks to valleys of 3–4 and 0.2 nm, respectively [7].

It is also of interest to tribologists and rheologists to measure the effect of the roughness characteristics on the lubricant film when the average thickness of the lubricant film remains constant. The model studied here is not an exact replica of the roughness of real surfaces where roughness is

 

TABLE I. Parameters for the intermolecular and intramolecular potentials.

| | | | | | | |
|---|---|---|---|---|---|---|
| Stretching potential $\phi(r)$[a] | | $k=51\,600\,\epsilon\sigma^{-2}$ | | $r_0=0.153$ nm | | |
| Bond angle potential $\phi(\theta)$[b] | | $k_\theta=868.6\,\varepsilon$ | | $\theta_0=109.53°$[a] | | |
| Torsional potential $\phi(\alpha)$[c] | $C_0=9.2789$ (kj/mol) | $C_1=12.1557$ | $C_2=13.1201$ | $C_3=-3.0597$ | $C_4=26.2403$ | $C_5=-31.4950$ |
| Lennard-Jones potential $\phi_{lj}$[d] | $\varepsilon/k_B=50.5$ K | $\sigma=0.4045$ nm | $\varepsilon_w k_B=202$ K | | | |

[a,b] $r_0$ and $\theta_0$ are taken from Ref. [11].
[c] Taken from Ref. [12].
[d] $\varepsilon/k_B$ and $\sigma$ are taken from Ref. [11].

randomly distributed on the surface. However, it is constructive to quantify the ''roughness'' by few simple parameters that can make the final analysis clearer.

We will investigate the boundary condition of the flow in molecularly thin films of alkanes with roughness modeled by a sinusoidal wall. In Sec. II we will explain the simulation details of our model. The results for boundary conditions will be presented in Sec. III. In Sec. IV we will present the effect of the wall roughness on the properties of the lubricating film.

## II. SIMULATION DETAILS

A molecular-dynamics simulation is made for the study of thin liquid films confined between two sinusoidal atomic walls. The lubrication process is simulated as a Couette shear flow by moving the walls in opposite directions.

### A. The walls

Each wall is comprised of three layers of atoms of a bcc (body-centered-cubic) lattice. The position of the wall particles in the $Z$ direction is displaced by $\Delta z$ according to

$$\Delta z = A \sin(2\pi x/P), \tag{1}$$

where $A$ and $P$, which characterize the roughness, are, respectively, the amplitude and period of the sinusoidal wall.

Each atom on the wall is attached by a stiff spring to its lattice position. The wall springs have a potential of the form

$$\phi_s = \tfrac{1}{2} k_w R^2, \tag{2}$$

where $k_w$ is the spring stiffness and $R$ is the distance of the wall atom from its lattice site. Here a stiff spring with $k_w = 6000\varepsilon\sigma^{-2}$ is used, where $\sigma$ and $\varepsilon$ are the length and energy parameters for alkanes given in Table I. Periodic boundary conditions are applied in the $x$ and $y$ directions only. To keep consistent with the periodicity, the length of the simulation box in the $x$ direction should be chosen in such a way that it accommodates an integer number of full sinusoidal waves depending on the period ($P$).

### B. Model liquid

The simulated liquid is a model alkane. In most of the simulations, the liquid is composed of model hexadecane ($C_{16}H_{34}$) molecules. However, in some cases shorter chains of alkane molecules are used in the simulations. A united atom model is used to model the molecules, where $CH_2$ and $CH_3$ groups as interaction sites connected together making a chain. Figure 1 shows a 3D picture of a hexadecane molecule. The Lennard-Jones (LJ) potential given by Eq. (3) (below) governs the interactions of the atoms belonging to different molecules and also for the atoms on the same molecule separated by more than three atoms,

$$\phi_{\mathrm{LJ}}(r) = 4\varepsilon\left[\left(\frac{\sigma}{r}\right)^{12} - \left(\frac{\sigma}{r}\right)^{6}\right] - \phi_{\mathrm{shift}},$$
$$\phi_{\mathrm{shift}} = 4\varepsilon\left[\left(\frac{\sigma}{r_c}\right)^{12} - \left(\frac{\sigma}{r_c}\right)^{6}\right]. \tag{3}$$

The interaction between the wall atom and fluid molecule interaction sites is also governed by Eq. (3) with the wall length parameter $\sigma_w = \sigma$ but with $\varepsilon$ replaced by $\varepsilon_w$, which governs the strength of interaction between the walls and the fluid. Here $\varepsilon_w = 4\varepsilon$ is used, which is close to a typical surface energy of metals. For the gold surface, $\varepsilon_w$ is about 220 K [10], and for other metal surfaces typical values in the same range can be used.

Intramolecular architecture including bond stretching, angle bending, and torsional potentials are included in the model. These potentials are given, respectively, by the following equation:

$$\phi(r) = \tfrac{1}{2} k (r_{ij} - r_0)^2, \tag{4}$$

$$\phi(\theta) = \tfrac{1}{2} k_\theta (\cos\theta - \cos\theta_0)^2, \tag{5}$$

$$\phi(\alpha) = \sum_i^5 C_i (\cos\alpha)^i. \tag{6}$$

The parameters for the intramolecular and also intermolecular potentials are given in Table I.

Figure 2 shows a snapshot taken from the simulation box for a typical simulation with hexadecane molecules. The average thickness of the film, which remains constant during the simulation, is measured from the average position of the first layer of the sinusoidal wall as shown in the figure. However, the actual film thickness varies as the crests and valleys pass each other as the walls are traveling in the opposite

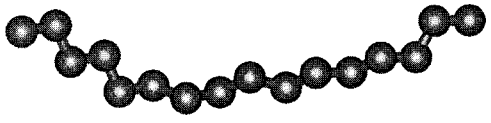

FIG. 1. A 3D picture of a hexadecane molecule.

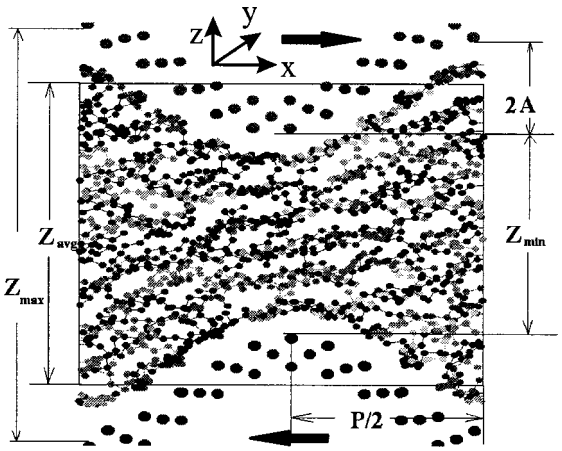


FIG. 2. A snapshot of the simulation box for the simulation of Couette shear flow by using a sinusoidal wall. The sheared liquid in this snapshot is hexadecane. The segments of the same molecule are shown by the same shade for clarification.

direction. The thickness of the film varies between maximum and minimum values shown by $Z_{\max}$ and $Z_{\min}$, where

$$Z_{\max}=Z_{\text{avg}}+2A,$$
$$Z_{\min}=Z_{\text{avg}}-2A. \tag{7}$$

Several simulations have been conducted to obtain the averaged velocity profiles for many different parameters including the amplitude ($A$) and period ($P$) of the sinusoidal wall and also the size of the fluid molecules. The volume of the fluid in the simulation box, however, remains constant and is calculated from the average thickness ($Z_{\text{avg}}$). The simulations are conducted at extreme pressures and high temperatures typical of conditions one expects in some real lubrication problems.

The average density of the fluid is calculated from

$$\rho_{\text{av}}=\frac{mN_f}{Z_{\text{avg}}\times X\times Y}, \tag{8}$$

where $m$ is the mass of each molecular segment, which is taken to be that of $CH_2$ (14.152 amu), $N_f$ is the number of fluid molecule segments, and $X$ and $Y$ are the dimensions of the simulation box in the $x$ and $y$ directions. The average density for the simulations here was $2.288\sigma^{-3}$ (810 kg/m$^3$).

These simulations have been conducted in isothermal conditions at $T=9.46\varepsilon/k_B$ (478 K). The thermal part of the velocities of the wall and fluid particles is rescaled every few time steps in all three directions [5]. The pressure depending on the thickness and other parameters ranges from 600 to 1000 MPa.

To calculate the local properties such as the streaming velocity profiles and local-density profiles, we have used a slicing technique method which is described in detail elsewhere [5,4]. Equations of motion were integrated by a leap-frog Verlet algorithm. The time step used in the simulation was 0.002 in reduced units. An equilibrium run of 100 000 time steps was performed followed by another 200 000 time steps to collect the results.

Simulations are performed by a domain decomposition parallel algorithm [13] on a cluster of DEC Alpha 500/286 workstations by using PVM (parallel virtual machine) message passing software that provided good speedup and efficiency.

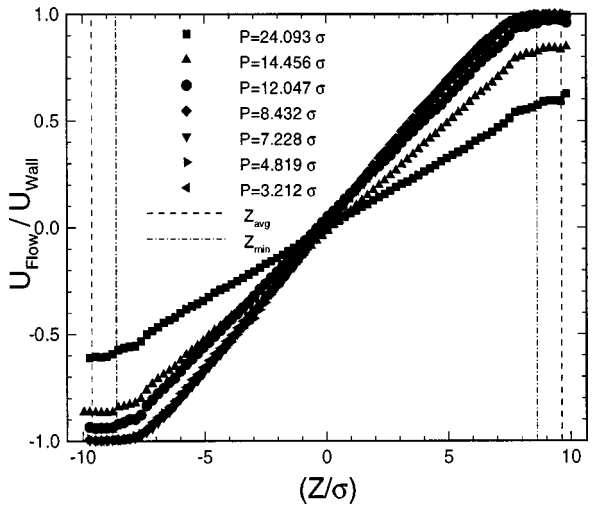


FIG. 3. Velocity profiles for an average film thickness of 7.8 nm ($19.275\sigma$) for various film periods of a sinusoidal wall ranging from 9.75 to 1.3 nm. The dashed line and dash-dotted line show the average and minimum film thickness positions. For all the simulations $A=0.4045$ nm ($1\sigma$).

## III. RESULTS

Our emphasis in this paper is to obtain some results to see how certain characteristics of surface topography and also fluid particle size correlate with boundary conditions. Here with a sinusoidal wall two important geometric parameters, namely the amplitude ($A$) and period ($P$) of the sinusoidal wall, will be examined to see what effects these two parameters have on the boundary condition. These two parameters are an indication of size and frequency of roughness on the surface. We have calculated velocity profiles and density profiles for many different cases and the results are used for

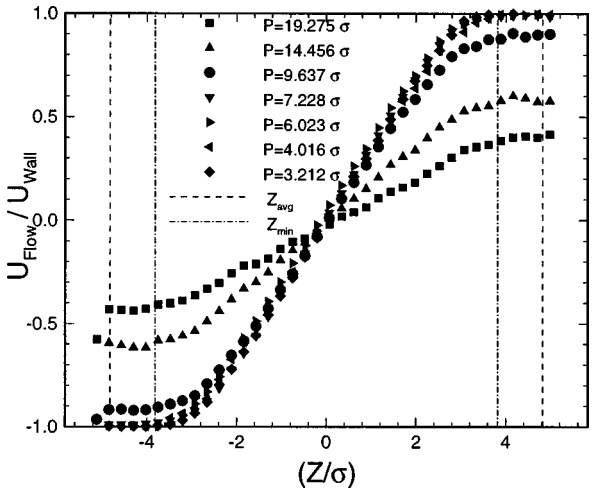


FIG. 4. Velocity profiles for an average film thickness of 3.9 nm ($9.637\sigma$) for various periods of a sinusoidal wall ranging from 7.8 to 1.3 nm. The dashed line and dash-dotted line show the average and minimum film thickness positions. For all the simulations $A=0.4045$ nm ($1\sigma$).

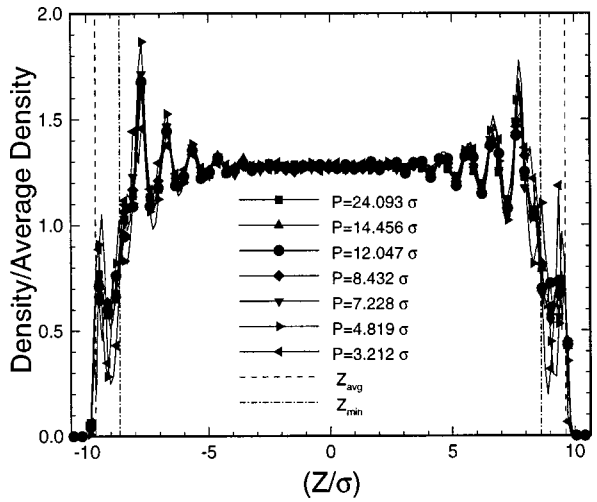


FIG. 5. Density profiles for the same simulations described in Fig. 3. Dashed line and dash-dotted line show the average and minimum film thickness.

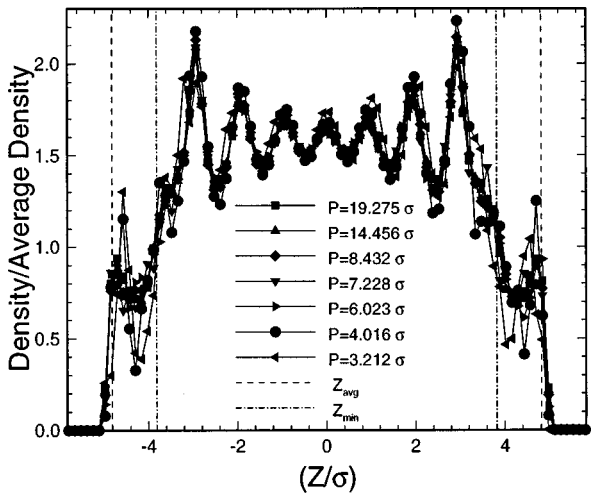


FIG. 6. Density profiles for the same simulations described in Fig. 4. Dashed line and dash-dotted line show the average and minimum film thickness.

the discussions. The velocity profiles are shown as the ratio of the flow velocity to the wall velocity, so that a value of 1 on the wall means there is no slip. A value less than 1 shows there is some slip on the wall. For all the simulations here, we have used a shear rate $\dot{\gamma}=0.245\,(\varepsilon/m\sigma^2)^{1/2}\,(10^{11}\,\mathrm{s}^{-1})$.

### A. Effect of the period (*P*) on the slip

To study the effect of the period of the roughness, we used hexadecane molecules for the simulation. The length of the hexadecane molecule is about 1.8 nm ($4.32\sigma$). We have performed simulations for different values of the period $P$ ranging from many times the length of the hexadecane molecule to values about equal to the hexadecane molecule length. For this series of simulations, the amplitude of roughness ($A$) is kept constant at $A=0.4045$ nm ($1\sigma$). The simulations are conducted for two films with average thickness of $Z_{\mathrm{avg}}=7.8$ nm ($19.275\sigma$) and $Z_{\mathrm{avg}}=3.9$ nm ($9.637\sigma$). The velocity profiles obtained for these two films are displayed in Figs. 3 and 4.

The effect of the period of roughness can be seen from the results. In both film thicknesses simulated here it can be seen that slip on the wall increases as we increase the roughness period. However, it can also be seen that the slip at the boundary only starts to appear when we increase $P$ to greater than a certain limit. For a film thickness of 3.9 nm ($9.637\sigma$), it seems that the onset of slip is at values around $P=3.6-4$ nm ($9-10\sigma$). This is about twice the length of the hexadecane molecule. From Fig. 4 it can be seen that there is no slip for $P\geqslant 5.85$ nm ($14.456\sigma$). For a thicker film of 7.8 nm ($19.275\sigma$) in Fig. 3 we can see that the onset of slip is at lower values of $P$ around 4.87 nm ($12\sigma$). It can be seen that for the same value of $P=5.85$ nm ($14.456\sigma$) for the film thickness of 3.9 nm, the amount of slip on the wall is about 0.4 times the wall velocity. It is about only 0.15 for the same value of $P$ for a thicker film of 7.8 nm. It is already established that for these ultrathin films, the amount of slip is increased as we decrease the film thickness [5,14]. This effect seems to be independent of the wall structure as with soft walls [5] and hydrocarbon tethered walls [14] and here with sinusoidal rough walls one gets the same result.

The dependence of slip on the period of roughness is explainable by the way the fluid molecules interact with the wall. We have obtained the local-density profiles for the same thicknesses and they are displayed in Figs. 5 and 6.

It can be seen from those figures that the density profiles are similar to those typical of inhomogeneous films. Between two dashed-dotted lines, which represent the minimum thick-

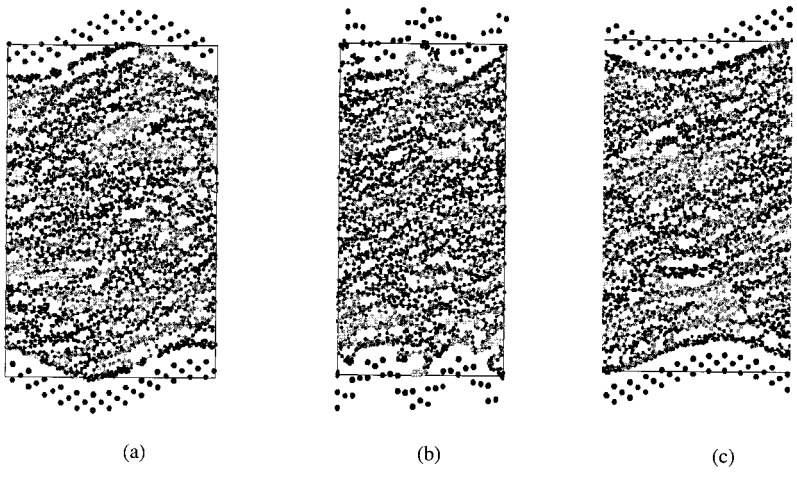


FIG. 7. Snapshots in the *xz* plane for three different values of (a) $P=5.85$ nm, (b) $P=3.41$ nm, and (c) $P=1.95$ nm. For all the simulations $A=0.4045$ nm.

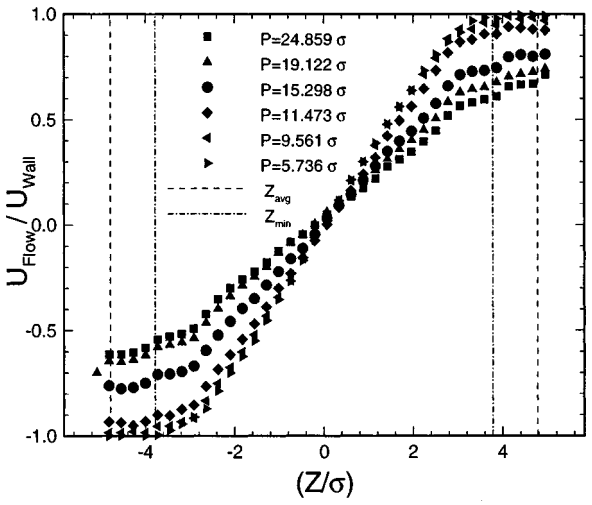


FIG. 8. Velocity profiles for various values of $P$ for a film consisting of $C_8H_{18}$ molecules. Average film thickness is 3.9 nm and amplitude of roughness $A=0.4045$ nm.

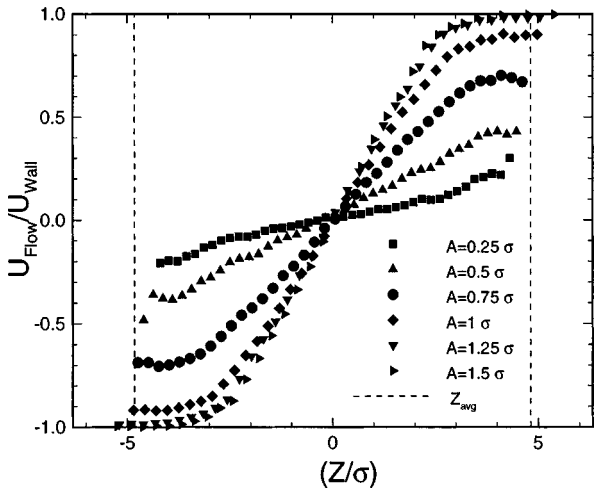


FIG. 9. Velocity profiles for an average film thickness of 3.9 nm ($9.637\sigma$) for various amplitudes of a sinusoidal wall ranging from 0.1 to 0.61 nm. The dashed line shows the average film thickness position. For all the simulations $P=3.9$ nm ($9.637\sigma$).

ness area, there is a peak immediately next to the walls and then a few other smaller peaks that damp down toward the center of the film. The density profiles in the central part of the film are almost the same for all the values of $P$. However, it seems that as $P$ is decreased, the peaks close to the wall get slightly higher. It also seems that the molecular concentration in the area between the minimum thickness line and the average thickness line is also important in determining the degree of slip. It can be seen that for lower values of $P$, the peaks are stronger in this area. It is in this area where molecules trap between crests and valleys of the sinusoidal wall. Figure 7 shows three snapshots in the $xz$ plane for a film thickness of 7.8 nm with different periods for roughness. It is more likely for a fluid molecule to become trapped between the valley and crest of the wall for lower values of the period. Close investigation of the snapshots in other planes has shown that these trapped molecules tend to lie down normal to the direction of flow with their backbone parallel to the $y$ axis, which is geometrically the natural position at which they can relax.

However the slip is dependent on the film thickness, the dependence of the slip on $P$ seems to be correlated with the length of the fluid molecule. To establish a correlation between the onset of slip and a relevant ratio of the molecule length and $P$ on a certain film thickness, we have also conducted a series of simulations for a shorter molecule, namely octane $C_8H_{18}$, that has only eight segments on the chain. The length of this molecule is 0.75 nm. The simulations are performed for the same average film thickness of 3.9 nm, over various values of $P$. The results are shown in Fig. 8.

If we compare the velocity profiles in this figure with those in Fig. 4 for hexadecane, we can see that the onset of slip is at higher values of $P$. For hexadecane for $P=7.9$ nm, the slip on the wall is about 60% of the wall velocity while for a similar value of $P$ for $C_8H_{18}$ slip is only 30% of the wall velocity. It seems that the onset of slip for $C_8H_{18}$ is at values between 4.6 and 5 nm ($11.3\sigma$), which is larger than what was observed for hexadecane. This is about six times the length of the $C_8H_{18}$ molecule.

This means that the length of the molecules is an important factor in determining the boundary condition. In order to study this, we have conducted further simulations that will be presented in the upcoming sections.

### B. The effect of roughness amplitude on slip

Another important factor of the surface topology is the amplitude of the asperities. In our sinusoidal wall model it is given by the amplitude ($A$). We have chosen a film thickness of 3.9 nm ($9.637\sigma$) and a period of roughness of 3.9 nm ($9.637\sigma$). The simulated fluid is hexadecane. The velocity profiles for different values of $A$ are depicted in Fig. 9. Dashed lines here show the position of the average film thickness, which was the same for all the simulations. The position of the minimum film thickness, however, was different because different amplitudes were used in the simulations so that we have not displayed the minimum film thickness position here. From the results it is obvious that the amplitude of the roughness has a profound effect on the degree of the slip on the wall. It can be seen that the slip is substantial at $A=0.1$ nm ($0.25\sigma$), amounting to about 0.7 times the wall velocity on the wall. This, however, is reduced as $A$ is increased further and a nonslip condition is established at about 0.51 nm ($1.25\sigma$). Studying the density profiles also reveals some information about the effect of the roughness amplitude. For the same systems as described in Fig. 9, density profiles are displayed in Fig. 10.

It can be seen that as we increase the amplitude, the density in the middle region is increased. The peak density near the walls is also moved inward. These are, however, the direct results of having an effectively thinner minimum thickness ($Z_{\min}$) film as the amplitude is increased and the average film thickness is kept constant.

Three snapshots taken from the simulation box for various values of $A$ are shown in Fig. 11. It can be seen that with the smallest value of $A=0.1$ nm, the wall is effectively like a flat wall and the observed slip is the largest. At higher values of amplitude, fluid chains are trapped in the valleys and effec-

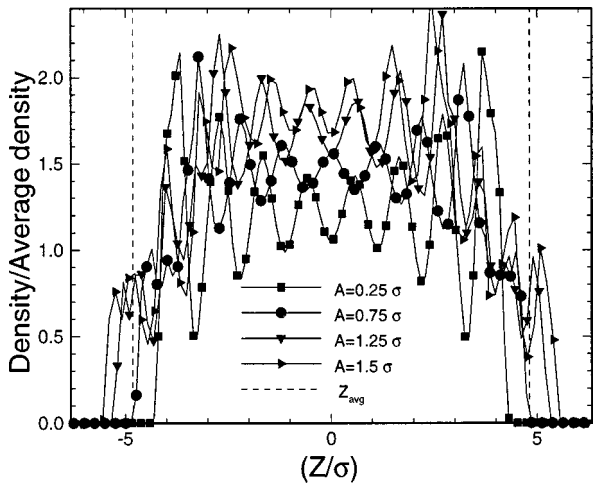


FIG. 10. Velocity profiles for an average film thickness of 3.9 nm ($9.637\sigma$) for various amplitudes of a sinusoidal wall ranging from 0.1 to 0.61 nm. For all the simulations $P=3.9$ nm ($9.637\sigma$).

tively transfer the wall momentum to the rest of the fluid in the middle part.

### C. The effect of the length of the fluid molecules

We already observed in Sec. III A that the size of the fluid molecules is important in determining the boundary condition. To further study this effect, we conducted many other simulations with molecules with different sizes. All these molecules have the same structure characteristics as hexadecane as described in Table I. However, the number of segments on the chain is different. Here we have examined molecules with 4, 5, 6, 8, and 16 segments. The density of the fluid is the same, $2.288\sigma^{-3}$ (810 kg/m$^3$), making the results comparable. Also, we have the same temperature as was used for hexadecane. For all the simulations here, the amplitude of roughness $A=0.2$ nm ($0.5\sigma$). Although the thickness and period of roughness used are slightly different for these molecules, the difference is negligible considering the effects of those parameters on the slip. These values are included in Table II. This difference is due to the technical difficulty of obtaining the same density with a different number of molecules.

It can be seen from the velocity profiles in Fig. 12 that the slip is clearly getting larger as the length of the molecules increases. The least slip happens for $C_4H_{10}$, where only about 10% slip is observed on the wall, and as the length of the fluid molecules is increased, the amount of slip increases and for hexadecane it can be seen that the slip on the wall is as much as 50–60% of the wall velocity.

TABLE II. Average film thickness and period of roughness used for various length molecules.

| Molecule | $C_4H_{10}$ | $C_5H_{12}$ | $C_6H_{14}$ | $C_8H_{18}$ | $C_{16}H_{36}$ |
|---|---|---|---|---|---|
| $Z_{avg}$ ($\sigma$) | 10.62 | 9.81 | 10.62 | 9.56 | 9.64 |
| $P$ ($\sigma$) | 10.62 | 9.81 | 10.62 | 9.56 | 9.64 |
| Molecular Length (nm) | 0.375 | 0.5 | 0.62 | 0.87 | 1.75 |

This effect can be explained by the fact that as the molecular length is increased while the size of the roughness in terms of the amplitude and periodicity remains constant, it gets more difficult for the molecules to accommodate themselves between the crests and valleys on the wall. This situation causes an increased slip at the wall that was seen here. However, in examining the density profiles for different length molecules, not much difference is found. Figure 13 shows the density profiles for $C_8H_{18}$ and $C_{16}H_{34}$, for which the simulations are conducted at almost the same thickness and roughness period. It can be seen that the density profiles are almost identical.

One of the other important structural properties is the orientation of the chains with respect to the walls. To investigate this, the square of the direction cosine ($\cos\theta_z$) of the bond vectors with respect to the $Z$ axis (normal to the wall) was measured and its MD average was calculated over all the molecules and their bonds and over time. For brevity, we call $(\cos\theta_z)^2$ the orientation factor. A value close to zero for $(\cos\theta_z)^2$ is an indication that bonds are oriented close to parallel with respect to the walls, and a value close to 1 shows that the bonds are mostly normal to the walls. The results for $(\cos\theta_z)^2$ are shown in Fig. 14 for various molecular lengths.

It can be seen that as the length of the molecule increases, the orientation of the bond becomes more parallel with the $X$ axis. Of course one might argue that the decrease in the orientation factor is partly due to the different actual shear rates that the fluid experiences with different degrees of slip.

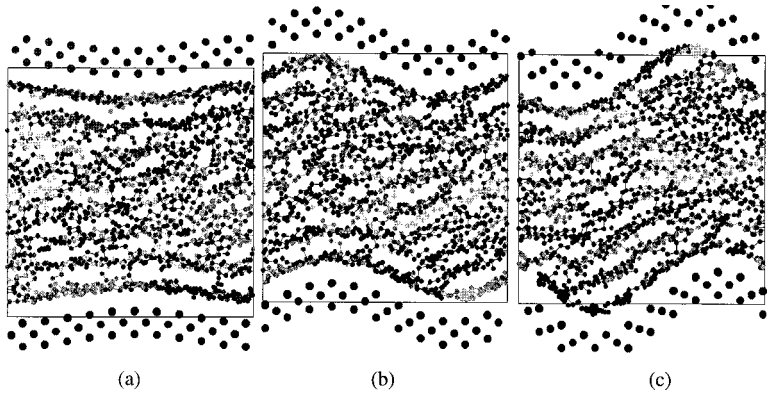


FIG. 11. Snapshots from the simulation box in the $xz$ plane for three different values of roughness amplitude (a) $A=0.1$ nm, (b) $A=0.30$ nm, and (c) $A=0.51$ nm. Average film thickness for all the cases is $Z_{avg}=3.9$ nm and period of roughness is $P=3.9$ nm.

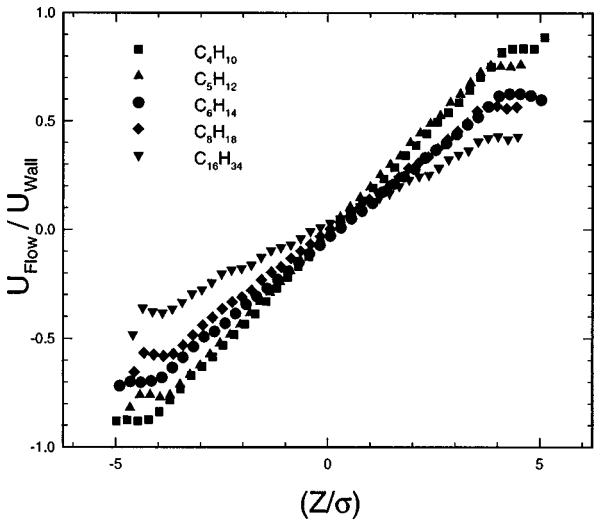


FIG. 12. Velocity profiles for various length alkane molecules. The amplitude of roughness for all the cases was 0.2 nm (0.5 $\sigma$).

In the MD simulations with flat soft atomic walls [5], it is been shown that the orientation factor actually decreases as the shear rate is increased. Having a higher degree of slip for longer chains means that they experience lower actual shear rates. This means that at actual shear rates similar to what is experienced by a shorter chain, they would give even lower values for $(\cos\theta_z)^2$. This is an indication that the bond orientation for shorter molecules is more strongly normal to the walls.

## IV. RHEOLOGICAL PROPERTIES OF THE LUBRICANT FILM

From the engineering point of view, one of the important characteristics to be measured is the rheological properties of the lubricant film. For the simulations conducted here, we have measured many important properties of the film including viscosity, normal stress differences, and normal pressure for various surfaces with different roughness characteristics. We will investigate the effect of the amplitude and period of roughness with the particular model that we have used here on these properties. For the simulations conducted here, *n*-hexadecane is used as the lubricant.

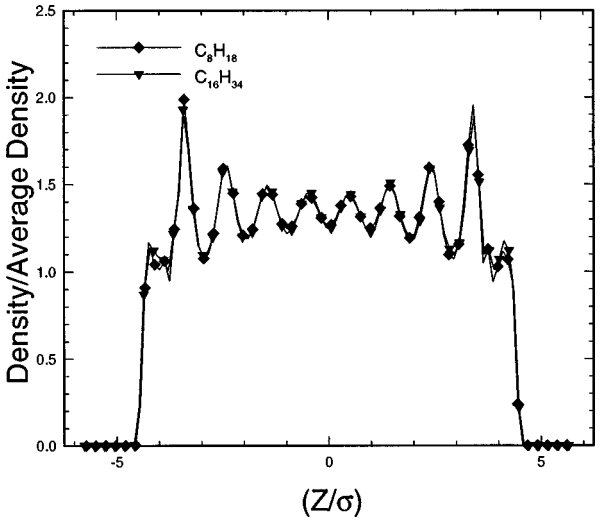


FIG. 13. Density profiles for two different length alkanes. $A = 0.2$ nm ($0.5\sigma$) for both cases.

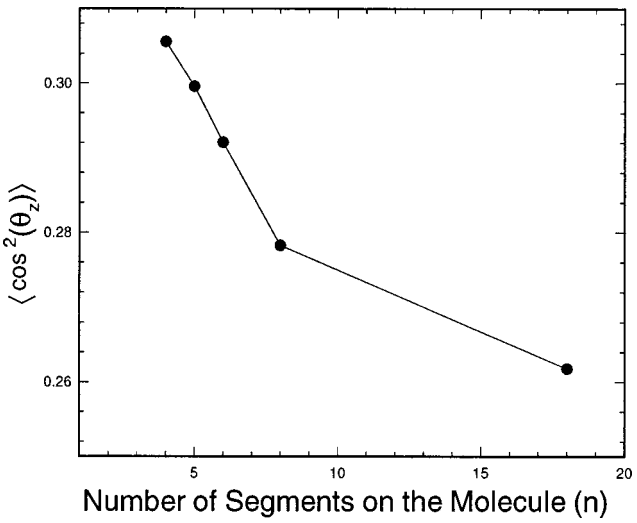


FIG. 14. Average orientation factor of the bonds with respect to the $Z$ axis for various molecular lengths given by the number of segments in each molecule.

### A. Stress tensor

Stress tensor components were found for a microscopic system of particles by the Irving-Kirkwood (1950) method. According to this method, the contribution of each particle to the stress tensor is in two parts, a configuration part and a kinetic part. This can be written as

$$\sigma_{\alpha\beta} = -\frac{1}{V}\left\langle \sum_{i}^{N} m_i u_{i\alpha} u_{i\beta} + \sum_{i}^{N} \sum_{j>i}^{N} \mathbf{r}_{ij\alpha} \mathbf{F}_{ij\beta} \right\rangle . \qquad (9)$$

The first sum on the right-hand side of Eq. (9) denotes the kinetic contribution where $m_i$ is the atomic mass and $\alpha$ and $\beta$ are coordination system axes which for a Cartesian system can be simply substituted by $X$, $Y$, or $Z$, and $u_{i\alpha}$ and $u_{i\beta}$ are the peculiar velocity components of particle $i$ in the $\alpha$ and $\beta$ directions. The second sum represents the configuration or potential contribution, where $\mathbf{r}_{ij\alpha}$ is the $\alpha$ component of the distance vector between particles $i$ and $j$ and $\mathbf{F}_{ij\beta}$ is the $\beta$ component of the force exerted on particle $i$ by particle $j$. We have to exclude the mean flow velocity when we consider the laboratory velocity component of a particle in the flow direction. Then for shear stress we can rewrite Eq. (9) as

$$\sigma_{xz} = -\frac{1}{V}\left\langle \sum_{i}^{N} m_i u_{iz}[u_{ix} - U_{x,i}] + \sum_{i}^{N} \sum_{j>i}^{N} \mathbf{r}_{ijz} \mathbf{F}_{ijx} \right\rangle , \qquad (10)$$

where $U_{x,i}$ is the average flow velocity at the position of particle $i$. The angular brackets denote the time average.

Shear stress can also be computed from the time average of the force in the $X$ direction applied to the wall particles by a fluid particles during the simulation. Then we calculated the shear stress by dividing this force by the projected area of the walls. This shear stress is given by Eq. (11),

$$\sigma_{xz,w}=\sum_{i}^{N_w}\sum_{j}^{N_F}\mathbf{F}_{x,ij}/A. \tag{11}$$

Normal stress in the $z$ direction can also be calculated from the force on the wall particles,

$$\sigma_{zz,w}=\sum_{i}^{N_w}\sum_{j}^{N_F}\mathbf{F}_{z,ij}/A. \tag{12}$$

In Eqs. (11) and (12), $\mathbf{F}_{x,ij}$ and $\mathbf{F}_{z,ij}$ are the forces in the $x$ and $z$ directions on a wall particle from the fluid particles. In the results presented here Eqs. (11) and (12) are used for the calculation of shear stress ($\sigma_{xz}$) and normal stress in the $z$ direction ($\sigma_{zz}$). For other components of the stress tensor we have used Eq. (9). Total pressure is calculated as the average of three normal pressure components.

### B. Viscosity and material functions

The shear rate is slightly different at different distances from the wall because the gradient of the velocity is not constant along the $z$ axis, therefore the local viscosity will be slightly different. More useful is the average over the whole width of the slit. Thus we use the following constitutive equation to find the viscosity:

$$\eta=\frac{\sigma_{xz}}{\dot{\gamma}}. \tag{13}$$

The first and second normal stress differences are

$$\begin{aligned} N_1&=\sigma_{xx}-\sigma_{zz},\\ N_2&=\sigma_{zz}-\sigma_{yy}. \end{aligned} \tag{14}$$

### C. The effect of the roughness amplitude ($A$)

For a tribologist or rheologist, the observable effects of the roughness on the lubricant properties have significant importance. As we saw in Sec. III B, the amplitude of the roughness has a direct effect on the slip and hence on the actual shear rate experienced by the lubricant film. In order to make the results comparable for the various values of $A$, we have used only values for $A$ that result in nonslip boundary conditions. Here the results will be presented for $A$ ranging from 0.4642 to 0.809 nm. The average film thickness used here is 3.898 nm and the applied shear rate is $10^{11}\,\mathrm{s}^{-1}$.

The results for the viscosity are shown in Fig. 15. It can be seen that the viscosity is an increasing function of the amplitude of roughness. The reason can be explained by the variation in the film thickness. For these series of simulations, the average film thickness is 3.98 nm. However, the maximum and minimum film thickness varies with the period of roughness according to Eqs. (7). Here with the average film thickness, the maximum and minimum film thickness ranges are $Z_{\max}=4.828-5.516\,\mathrm{nm}$ and $Z_{\min}=2.968-2.280\,\mathrm{nm}$. We have investigated the effect of the film thickness for hexadecane film in our previous work [5]. The results show an enhanced viscosity in the very thin film. The onset of this enhancement is at a film thickness about 1 nm. However, in those simulations the density of the films remains constant. In the current simulation, as we saw in Sec. III B, there is an increased density in the middle of the film as we increase the amplitude of roughness. These we suspect contribute to the increase of viscosity. Should the viscosity be a linearly decreasing function of thickness, since the film thickness varies periodically, the time average viscosity would be equal to the viscosity of a film with average thickness. However, since the viscosity enhances dramatically only for films thinner than 3.898 nm and remains almost the same for thicker films (i.e., the relationship is nonlinear), the viscosity of the minimum film thickness is determining in the time-average viscosity of the whole film. This results is an overall enhancement of the viscosity with increasing amplitude and it is more dramatic at larger values of $A$. We have also measured the first normal stress difference $N_1$ for the same simulations that are shown in Fig. 16.

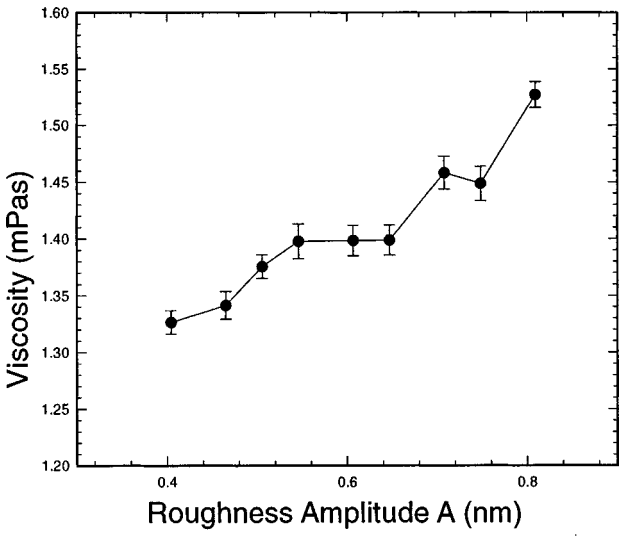


FIG. 15. Viscosity against the amplitude for a film of hexadecane. The film thickness is 3.898 nm and the shear rate is $10^{11}\,\mathrm{s}^{-1}$. For all the simulated points the period of roughness $P=3.898\,\mathrm{nm}$.

It can be seen that $N_1$ increases first and then drops as we increase the amplitude. Figure 17 shows the normal pressure as a function of the amplitude. It shows that $P_{zz}$ is an increasing function of $A$. The results shows that the trend is the same for two other normal stresses. That means the total pressure increases with $A$. So a decrease in $N_1$ for the larger values of amplitude shown in this region $\sigma_{xx}$ does not increase at the same rate as $\sigma_{zz}$ does. This can be because of the orientation of the molecules and their tendency to orient themselves normal to the flow in the direction of the $y$ axis in between the peaks and valleys of the walls.

### D. The effect of the roughness period ($P$)

We also investigated the effect of the period of roughness on the properties of the film. Again we have used the same shear rate of $10^{11}\,\mathrm{s}^{-1}$ and an average film thickness of 3.898 nm. The amplitude of roughness for all cases is 0.4045 nm. Only cases with the nonslip boundary condition are used for comparison so that the lubricant film experiences the same actual shear rate. The results for viscosity are shown in Fig. 18.

It can be seen that the viscosity is largest for the lowest value of the period of roughness. For the rest of them, it remains pretty flat with only a jump for $P=1.949\,\mathrm{nm}$. Al-

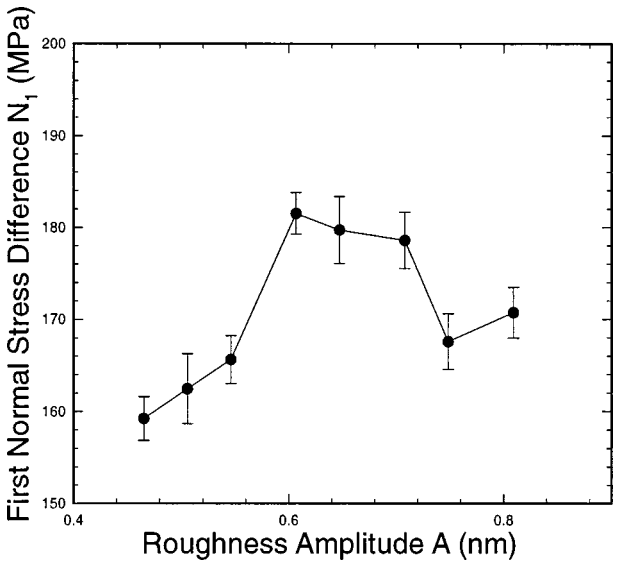


FIG. 16. First normal stress difference against the amplitude for a film of hexadecane. The film thickness is 3.898 nm and the shear rate is $10^{11}\,s^{-1}$. For all the simulated points the period of roughness $P=3.898$ nm.

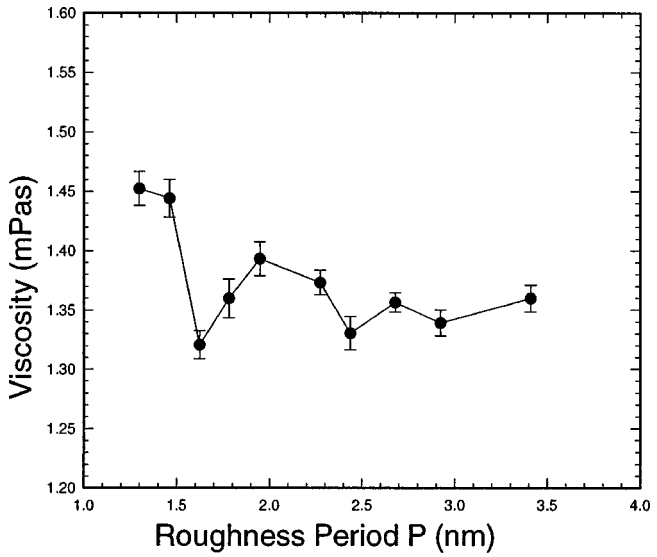


FIG. 18. Viscosity against the period of roughness for a film of hexadecane. The film thickness is 3.898 nm and the shear rate is $10^{11}\,s^{-1}$. For all the simulated points the amplitude of roughness $A=0.4045$ nm.

though the effect of the period of roughness is not very obvious on the viscosity, it has a clear effect on the first normal stress difference. It can be seen from Fig. 19 that $N_1$ increases and then remains constant as we increase the period. This trend can also be seen for the other properties that we have calculated here.

For the normal component of pressure $P_{zz}$ that is plotted against the period of roughness in Fig. 20, the trend is similar to that of viscosity. There is a peak in the lowest value of $P$ followed by a drop in $P_{zz}$ and a pretty flat region at larger values of $P$. Total pressure is shown in Fig. 21 and it can be seen that it decreases as $P$ is increased and then remains constant. From all these results it can be seen that for $P>2.437$ nm the properties of the film remain largely unchanged. This implies that $P$ is important only when it is comparable with the size of the molecules (in this case 1.8 nm for hexadecane). Beyond that, it seems $P$ has little or no effect on the film properties.

## V. CONCLUSIONS

Here we examined the effect of the wall roughness on the boundary condition and rheological properties of the lubricant. A sinusoidal wall model was used to study the effect of the size of asperities and their frequency on the wall slip. It was shown that as the period of roughness is increased, the degree of slip on the wall also increases. Also, we observed

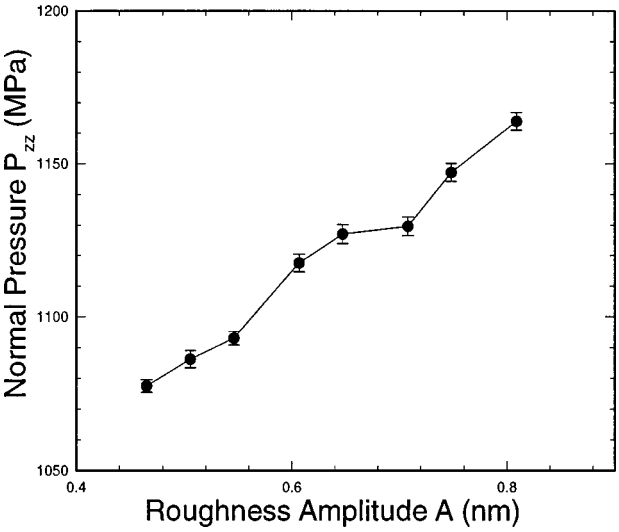


FIG. 17. Normal pressure ($P_{zz}$) perpendicular to the wall against the amplitude for a film of hexadecane. The film thickness is 3.898 nm and the shear rate is $10^{11}\,s^{-1}$. For all the simulated points the period of roughness $P=3.898$ nm.

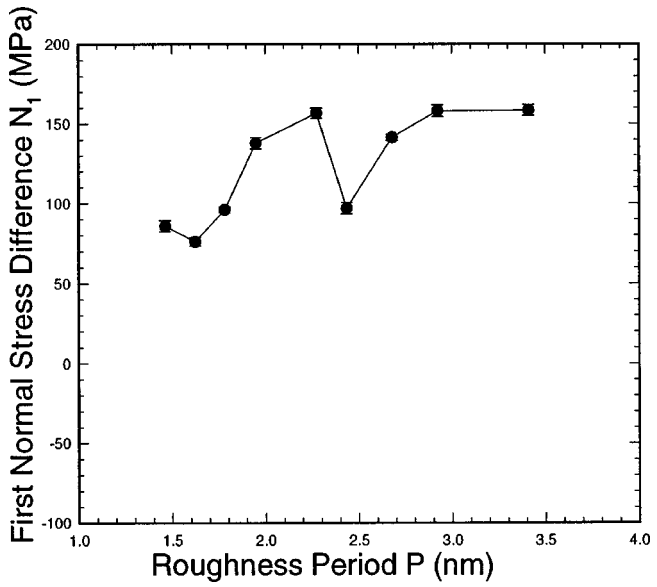


FIG. 19. First normal stress difference against the period of roughness for a film of hexadecane. The film thickness is 3.898 nm and the shear rate is $10^{11}\,s^{-1}$. For all the simulated points the amplitude of roughness $A=0.4045$ nm.

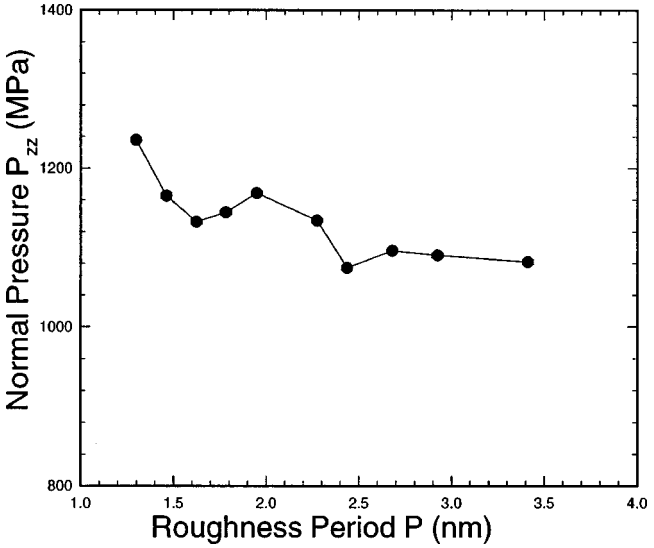


FIG. 20. Normal pressure in the direction normal to the wall $P_{zz}$ against the period of roughness for a film of hexadecane. The film thickness is 3.898 nm and the shear rate is $10^{11}\,s^{-1}$. For all the simulated points the amplitude of roughness $A=0.4045$ nm.

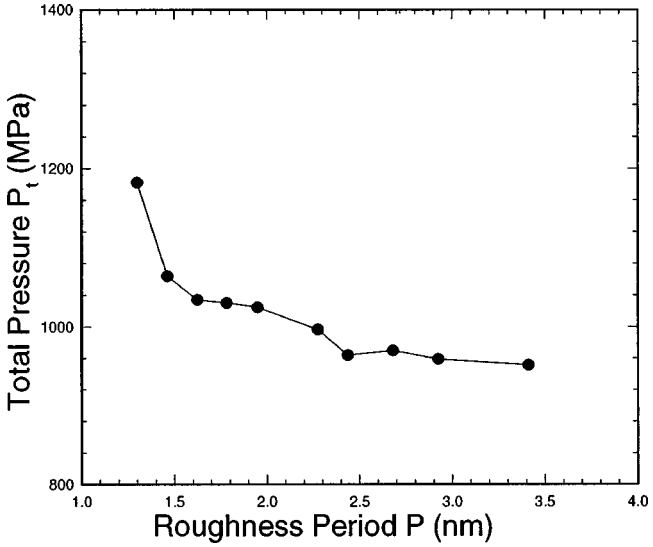


FIG. 21. Total pressure $P_t$ against the period of roughness for a film of hexadecane. The film thickness is 3.898 nm and the shear rate is $10^{11}\,s^{-1}$. For all the simulated points the amplitude of roughness $A=0.4045$ nm.

that with the larger roughness amplitudes it is possible to decrease the slip. It was also shown that with shorter molecules the amount of the slip would be dramatically lower.

These findings here confirm the theoretical prediction by Pearson and Petrie [9] at molecular dimensions. Our findings here give detailed insight into what happens at the molecular level in these ultrathin films. The effect of the geometrical characteristics of the surface are highlighted here and can have important implications in real engineering applications and in the design of surface characteristics for certain applications.

The experimental measurements for roughness of gold and mica surfaces in Ref. [7] correspond to $A=1.5-2$ and 0.1 nm in our simulations. Considering the results we obtained in Sec. III B with our simulation it seems that for a gold surface or other metallic surfaces which have even rougher surfaces (12–50 nm for heat treated steel [7]), a nonslip condition holds even at the high shear rates examined in our simulations. This conclusion is valid at least with relatively short alkane chains that we modeled here. For mica with a smooth surface the results suggest a slip boundary condition. However, since it has slightly higher surface energy than that examined here, the slip may be less. However, it seems that this matter should be considered more carefully in experiments with mica. The results here can be used in experiments in nanotribology and nanorheology to use proper materials for desired boundary conditions depending on the liquid film.

The investigation on the effect of these asperities on the rheological properties of these thin films also showed that there is a dramatic effect on the fluid viscosity and observed normal stress differences on the fluid properties. These effects are more dramatic with roughness amplitude demonstrated by enhancement in the film viscosity and observed normal stress differences and pressure. Also, for a period of roughness when it is comparable with the size of molecule, the effect is more obvious. However, at higher periods it seems the effect is minimal and small.

[1] D. Dowson, in *Proceedings of the 19th Leeds-Lyon Symposium on Tribology*, edited by D. Dowson (Elsevier, Amsterdam, 1992), pp. 3–12.
[2] A. Thompson and M. O. Robbins, Phys. Rev. A **41**, 6830 (1990).
[3] A. Thompson, G. S. Grest, and M. O. Robbins, Phys. Rev. Lett. **68**, 3448 (1992).
[4] A. Jabbarzadeh, J. D. Atkinson, and R. I. Tanner, J. Non-Newtonian Fluid Mech. **69**, 169 (1997).
[5] A. Jabbarzadeh, J. D. Atkinson, and R. I. Tanner, J. Non-Newtonian Fluid Mech. **77**, 53 (1998).
[6] A. Jabbarzadeh, J. D. Atkinson, and R. I. Tanner, J. Chem. Phys. **110**, 2612 (1999).
[7] M. Georges, S. Millot, J. L. Loubet, A. Tonck, and D. Mazuyer, in *Proceedings of the 19th Leeds-Lyon Symposium on Tribology* (Ref. [1]), pp. 443–452.
[8] S. Richardson, J. Fluid Mech. **59**, 707 (1973).
[9] J. R. A. Pearson and C. J. S. Petrie, in *Polymer Systems: Deformation and Flow*, Proceedings of the Annual Conference of the British Society of Rheology, edited by R. E. Wetton and R. W. Whorlow (Macmillan, London, 1968), pp. 163–187.
[10] T. K. Xia, Jian Ouyang, M. W. Ribarsky, and Uzi Landman, Phys. Rev. Lett. **69**, 1967 (1992).
[11] S. Chynoweth and Y. Michopoulos, Mol. Phys. **81**, 133 (1994).
[12] P. van der Ploeg and J. C. Berendsen, J. Chem. Phys. **76**, 3271 (1982).
[13] A. Jabbarzadeh, J. D. Atkinson, and R. I. Tanner, Comput. Phys. Commun. **107**, 123 (1997).
[14] S. D. Gupta, H. D. Cochran, and P. T. Cummings, J. Chem. Phys. **107**, 10 316 (1997).